Measurements of photon production at ATLAS

Ana Cueto, on behalf of the ATLAS Collaboration[*]

Laboratoire d'Annecy de Physique des Particules (L.A.P.P.)
E-mail: ana.cueto@cern.ch

Measurements of prompt-isolated photon production at hadron colliders provide a stringent test of perturbative QCD and can be used to constrain the gluon distribution functions inside the proton. In this article, the measurement of inclusive-photon cross-section ratio at $\sqrt{s} = 8$ and $\sqrt{s} = 13$ TeV is presented together with the isolated-photon plus jet cross section measurements at $\sqrt{s} = 13$ TeV. The measurements use proton-proton collision data collected by the ATLAS experiment at the LHC.

XXVII International Workshop on Deep-Inelastic Scattering and Related Subjects - DIS2019
8-12 April, 2019
Torino, Italy

---

[*]Speaker.

1. Introduction

Measurements of prompt photons represent a classical test of perturbative quantum chromo-dynamics (pQCD) with a hard colourless probe. Prompt photons necessitate an isolation criterion to avoid the large contribution of photons produced in hadron decays. After this requirement, the dominant production mechanism is the Compton scattering process, $qg \rightarrow q\gamma$. Therefore, direct-photon production provides new observables with independent information to constrain the gluon density inside the proton [1].

Comparisons of measurements of prompt-photon production with pQCD predictions are usually limited by the theoretical uncertainties associated to the missing higher-order terms in the perturbative expansion. The uncertainties on the next-to-leading order (NLO) pQCD predictions are larger than those of experimental nature, preventing a more precise test of the theory. A stringent test of the theory can be achieved either by the inclusion of the next-to-next-to-leading order (NNLO) QCD corrections in the calculation [2, 3] or by measuring the ratio of cross sections at different centre-of-mass energies.

Studies of the dynamics of the photon plus jet system are helpful to validate the description of the process provided by Monte Carlo (MC) generators. This is particularly useful for beyond the Standard Model searches involving photons in which these generators are used to estimate the Standard Model background. In this article, the measurement of inclusive-photon cross-section ratio at $\sqrt{s} = 8$ and $\sqrt{s} = 13$ TeV [4] is presented together with the isolated-photon plus jet cross section measurements at $\sqrt{s} = 13$ TeV [5]. Both measurements use proton-proton collision data collected by the ATLAS experiment at the LHC [6].

2. Ratio of cross sections for inclusive-isolated photon production at $\sqrt{s} = 8$ TeV and $\sqrt{s} = 13$ TeV

The cross sections ratio for inclusive isolated-photon production in pp collisions, $R^{\gamma}_{13/8}$, is measured with data collected by the ATLAS detector at $\sqrt{s} = 13$ and $\sqrt{s} = 8$ TeV as a function of E^{γ}_{T} in different regions of the photon pseudorapidity $|\eta^{\gamma}|$ for photons with $E^{\gamma}_{\mathrm{T}} > 125$ GeV and $|\eta^{\gamma}| < 2.37$, excluding the region $1.37 < |\eta^{\gamma}| < 1.56$.

Measurements of the cross section for isolated prompt-photon production were performed by ATLAS at 8 and 13 TeV with an integrated luminosity of 20.2 fb^{-1} and 3.2 fb^{-1} respectively. The measurement at 13 TeV was performed such as the ratio $R^{\gamma}_{13/8}$ could be easily measured: the phase-space region to which the data distributions were unfolded was the same as that at 8 TeV in what concerns the photon isolation and regions of $|\eta^{\gamma}|$; regarding the range in E^{γ}_{T}, the analysis at 13 TeV covers the range $E^{\gamma}_{\mathrm{T}} > 125$ GeV with the same binning used at 8 TeV. Additionally, the double ratio of $R^{\gamma}_{13/8}$ over the ratio of the fiducial cross section for Z boson production at 13 and 8 TeV ($R^{Z}_{13/8}$), $D^{\gamma/Z}_{13/8}$, is also measured. This ratio $D^{\gamma/Z}_{13/8}$ benefits from the complete cancellation of the uncertainty in the measured integrated luminosity. The ratio of the fiducial cross section for Z boson production, $R^{Z}_{13/8}$, was also measured by the ATLAS Collaboration in [7] with a value of 1.537 ± 0.001 (stat.) ± 0.010(syst.) ± 0.044 (lumi.).

The uncertainty arising from the photon energy scale is the dominant uncertainty in the inclusive-photon cross section measurements. To correlate properly both measurements, the uncertainty on

the photon energy scale at 13 TeV is re-estimated using the same decorrelation model used at 8 TeV. A total of 22 individual sources of uncertainty in the energy scale and resolution of the photon [8] are considered. Twenty of them are common to both centre-of-mass energies. The two additional sources considered only at 13 TeV are due to the change in the detector configuration and running conditions of the 13 TeV data-taking period. The different sources of uncertainty are taken as correlated except for the uncertainty in the overall energy scale adjustment using $Z \rightarrow e^+e^-$ events and the uncertainties specific to the 13 TeV measurement.

The other sources of experimental uncertainties are all conservatively treated as uncorrelated due to different reasons like the optimization of the photon identification for data taken at 13 TeV, different techniques used in the estimation of the uncertainties or different tunes used in the Monte Carlo generators. The total systematic uncertainty is typically 5%.

In the case of the double ratio, $D^{\gamma/Z}_{13/8}$, the uncertainties due to $R^Z_{13/8}$ are treated as uncorrelated to those of $R^\gamma_{13/8}$ excluding the luminosity uncertainty. The statistical (0.1%) and systematic (0.7%) uncertainties in $R^Z_{13/8}$ are dominated by the uncertainty in the lepton reconstruction and efficiency. The correlation between the small contribution of the electron energy scale and the photon energy scale uncertainties in $D^{\gamma/Z}_{13/8}$ is safely neglected.

The NLO in pQCD predictions for $R^\gamma_{13/8}$ are computed using the JETPHOX [9] program, which includes a full NLO QCD treatment of the direct and fragmentation contributions for the process $pp \rightarrow \gamma + X$. The renormalisation, factorisation and fragmentation scales are set to E^γ_T. The calculations are performed using several parameterisations of the proton PDFs and the BFG set II of parton-to-photon fragmentation function. The strong coupling constant $\alpha_s(m_Z)$ is set to the value assumed in the fit to determine the PDFs. For instance, in the case of MMHT2014, $\alpha_s(m_Z)$ is set to 0.120. A fixed-cone isolation criterion is applied at parton level. The total transverse energy of the partons inside a cone of radius $R = 0.4$ around the direction of the photon is required to be below $E^{\text{iso,cut}}_T = 4.2 \cdot 10^{-3} E^\gamma_T + 4.8$ GeV. Since the measurements refer to particle level, correction factors are estimated with PYTHIA to take into account the non-perturbative (NP) effects of hadronisation and underlying event. The correction factor applied to the parton-level predictions of $R^\gamma_{13/8}$ is $C^{\text{NP}}_R = 0.9964 \pm 0.0020$.

The theoretical predictions for $D^{\gamma/Z}_{13/8}$ are based on NNLO QCD calculations for $R^Z_{13/8}$ computed using the DYTURBO program, an optimised version the DYNNLO program [10], and the NLO QCD calculations for $R^\gamma_{13/8}$ described above. The calculations of both ratios use PDF sets extracted using NNLO QCD fits.

The sources of theoretical uncertainties considered are those due to the missing higher orders, the PDF- and α_s-induced uncertainties, the uncertainties due to the impact of the beam energy uncertainty and that on the non-perturbative effects. For $R^\gamma_{13/8}$, all the uncertainties are correlated between both centre-of-mass energy. In the case of $D^{\gamma/Z}_{13/8}$, the scale variations uncertainty is taken as uncorrelated between the different processes ratio. The total relative theoretical uncertainty is 2% (4 %) at low (high) E^γ_T in all regions of $|\eta^\gamma|$. For $|\eta^\gamma| < 1.37$, the uncertainty due to the PDFs can be as large as the contribution from the missing higher orders.

The measured values of $R^\gamma_{13/8}$ and $D^{\gamma/Z}_{13/8}$ are shown in Figure 1 for $|\eta^\gamma| < 0.6$. The measured $R^\gamma_{13/8}$ increases from approximately 2 at $E^\gamma_T = 125$ GeV to ~ 10 at the high-end of the spectrum. In the forward regions the increase of $R^\gamma_{13/8}$ with E^γ_T is larger than in the central region. At a fixed

value of E_T^γ, the measured ratio increases as $|\eta^\gamma|$ increases. Similar trends in the measured value of $D_{13/8}^{\gamma/Z}$ are observed.

The pQCD predictions are compared to the measurements and are found to be consistent within the reduced experimental and theoretical uncertainties. The theory predictions can reproduce the increase in E_T^γ and in $|\eta^\gamma|$. The significant reduction achieved in the experimental and theoretical uncertainties in the ratios allows a more stringent test of pQCD. The overall level of agreement between data and predictions in $R_{13/8}^\gamma$ ($D_{13/8}^{\gamma/Z}$) validates the description of the evolution of isolated-photon production (normalized to the Z boson production) in pp collisions with the centre-of-mass energy.
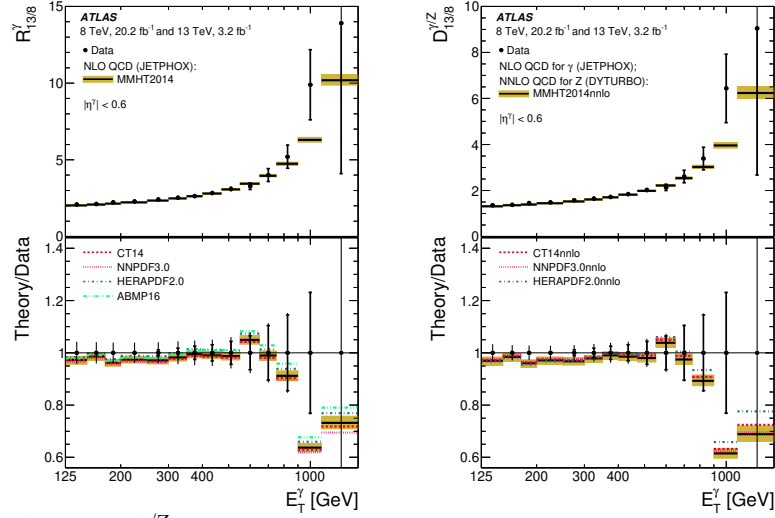

Figure 1: Measured $R_{13/8}^\gamma$ and $D_{13/8}^{\gamma/Z}$ (dots) as a function of E_T^γ for $|\eta^\gamma| < 0.6$ compared to pQCD predictions [4].

3. Measurement of the cross section for isolated-photon plus jet production in pp collisions at $\sqrt{s} = 13$ TeV using the ATLAS detector

This section describes the measurement of the differential cross sections for isolated-photon plus jet production using data collected at $\sqrt{s} = 13$ TeV by the ATLAS detector with a total integrated luminosity of 3.2 fb^{-1}. The measurements are presented as functions of the leading-photon transverse energy (E_T^γ), the leading-jet transverse momentum (p_T^{jet}), the azimuthal angular separation between the photon and the jet ($\Delta\phi^{\gamma-jet}$), the photon–jet invariant mass ($m^{\gamma-jet}$) and the scattering angle in the photon–jet centre-of-mass system ($|\cos\theta^\star|$). Tree-level plus parton-shower predictions from SHERPA and PYTHIA as well as next-to-leading-order QCD predictions from JETPHOX and SHERPA are compared to the measurements.

Photon identification is applied to suppress the background originated from neutral meson decays to photons within jets. It is mainly based on shower shapes in the calorimeter. Reconstructed photons are required to have transverse energies above 125 GeV and fall in the central region of the detector with $|\eta^\gamma| < 2.37$ excluding the calorimeter transition region $1.37 < |\eta^\gamma| < 1.56$. To further suppress the hadronic background, a calorimetric isolation criterion is applied. The transverse energy inside a cone of size $\Delta R = 0.4$ in the $\eta - \phi$ plane around the photon candidate, excluding the photon core is limited to be $4.2 \cdot 10^{-3} E_T^\gamma + 4.8$ GeV.

Jets are reconstructed using the anti-k_t algorithm with radius parameter $R = 0.4$. Spurious jet background is rejected by means of a jet-quality criteria. The leading jet is selected between those with a separation to the photon greater than $\Delta R = 0.8$ and is required to have a transverse energy larger than 100 GeV and rapidity $|y^{\text{jet}}| < 2.37$. For the measurements of the differential cross sections as functions of $m^{\gamma-\text{jet}}$ and $|\cos\theta^\star|$, the additional constraints $|\eta^\gamma| + |y^{\text{jet}-\text{lead}}| < 2.37$ and $m^{\gamma-\text{jet}} > 450$ GeV are imposed.

A residual background from jets misidentified as photons remains in the signal region after the identification and isolation requirements. This background is subtracted bin-by-bin employing a data-driven two-dimensional sideband method. The sideband background control regions are populated with photons that do not pass the signal identification or/and isolation requirements but satisfy a relaxed version of such criteria. After the background subtraction, the signal purity in the signal region is typically above 90%.

The cross sections are unfolded to the particle level in a region close to the applied event selection at reconstruction level described in the previous section. The main difference resides in the isolation requirement, which is $4.2 \cdot 10^{-3} E_{\text{T}}^\gamma + 10$ GeV at particle level. To perform the unfolding, LO Monte Carlo samples of the photon plus jet process are employed. Correction factors are estimated in each bin of the measurement that correct for the resolution effects and the efficiency of the photon and jet reconstruction. The correction factors vary between 1.08 and 1.21 depending on the observables.

The dominant sources of uncertainty are those on the jet and photon energy scale and that on the photon identification. The total systematic uncertainty is computed by adding in quadrature the uncertainties from all the sources considered. The size of the total systematic uncertainty goes from 4% to 10% depending on the observable and the phase-space region. The statistical uncertainty limits the precision of the measurement at high values of E_{T}^γ and $m^{\gamma-\text{jet}}$.

The NLO predictions of two programs, namely JETPHOX and SHERPA 2.2.2 [11], are computed. The settings of JETPHOX used to obtain the predictions are the same as explained in Section 2. Corrections for NP effects are applied to the calculations. Their values are close to unity within $\pm 5\%$ for the observables studied, except for $p_{\text{T}}^{\text{jet}-\text{lead}} \geq 600$ GeV where the factors can differ by up to 30% from unity. The SHERPA 2.2.2 program consistently combines parton-level calculation of the $\gamma + 1, 2$ jets at NLO accuracy and $\gamma + 3, 4$ jets at LO supplemented with parton shower while avoiding double-counting effects. The collinear divergencies coming from the fragmentation component are suppressed by imposing a smooth-cone isolation criterion. Uncertainties due to the missing higher-order terms, on α_{s} and the PDFs are considered. The uncertainty on the non-perturbative corrections is also taken into account in the JETPHOX predictions. The total uncertainty, in the case of JETPHOX (SHERPA), is 10-15% (15-25%) for most of the phase-space regions and are dominated by the terms beyond NLO.

The differential cross sections are presented in Figure 2 as functions of the observables studied. Values up to 1.5 (3.25) TeV in E_{T}^γ and $p_{\text{T}}^{\text{jet}-\text{lead}}$ ($m^{\gamma-\text{jet}}$) are accessed. The predictions of the fixed-order NLO QCD calculations based on the MMHT2014 PDF set and corrected by hadronisation and underlying event effects are compared to the measurements together with the predictions of the multi-leg NLO QCD plus parton-shower calculations of SHERPA based on the NNPDF3.0 PDF set. Both predictions describe the data within the experimental and theoretical uncertainties. Only the predictions of SHERPA are compared to the measured differential cross section as a function of the

$\Delta\phi^{\gamma-\text{jet}}$ since JETPHOX can only provide an effective LO description in the region outside the back-to-back configuration of the photon-jet system. The predictions were also obtained with different sets of the PDFs and differ by less than 5% with respect to the nominal ones. The recent calculations at next-to-next-to-leading order [1] shows an impressive improvement in the description of the observables studied in this analysis with a significant reduction of the theoretical uncertainties.
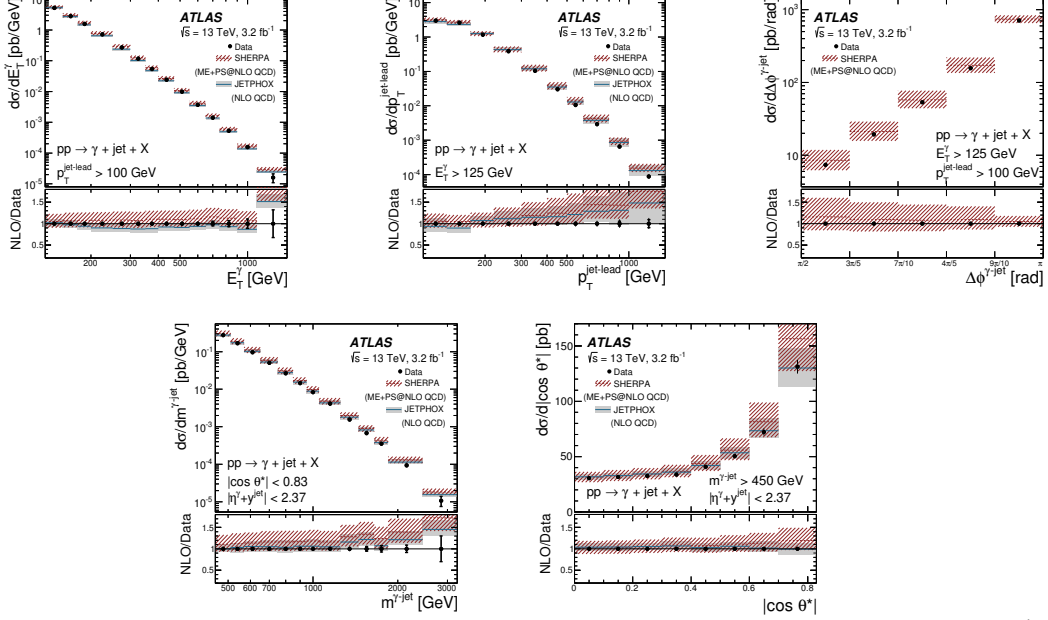

Figure 2: Measured cross sections for isolated-photon plus jet production as functions of E_T^γ, $p_T^{\text{jet}-\text{lead}}$, $\Delta\phi^{\gamma-\text{jet}}$, $m^{\gamma-\text{jet}}$ and $|\cos\theta^\star|$. The predictions from SHERPA (dashed lines) and JETPHOX (solid lines) are also shown [5].

Acknowledgement

References

[1] J. M. Campbell, J. Rojo, E. Slade and C. Williams, Eur. Phys. J. C **78**, no. 6, 470 (2018)

[2] X. Chen, T. Gehrmann, N. Glover, M. Höfer and A. Huss, [arXiv:1904.01044 [hep-ph]].

[3] J. M. Campbell, R. K. Ellis and C. Williams, Phys. Rev. Lett. **118**, no. 22, 222001 (2017)

[4] ATLAS Collaboration, JHEP **04**, 093 (2019)

[5] ATLAS Collaboration, Phys. Lett. B **780**, 578 (2018)

[6] ATLAS Collaboration, 2008 JINST 3 S08003

[7] M. Aaboud *et al.* [ATLAS Collaboration], JHEP **1702**, 117 (2017)

[8] ATLAS Collaboration, Eur. Phys. J. C **74**, no. 10, 3071 (2014)

[9] S. Catani *et al.*, JHEP **0205**, 028 (2002)

[10] S. Catani, L. Cieri, G. Ferrera, D. de Florian and M. Grazzini, Phys. Rev. Lett. **103**, 082001 (2009)

[11] E. Bothmann *et al.*, arXiv:1905.09127 [hep-ph].